JCRS Journal of Chemical Reactivity and Synthesis 2024: 14(4) 298-314

Research Article

Adsorption, Kinetics and Equilibrium Studies on Removal of Reactive Black 5 from Aqueous Solutions Using $ZnCo_2O_4$ Nano-spinel

Iman Khosravi*, Melika Eftekhar

Department of chemistry, Qe.c., Islamic Azad University, Qeshm, Iran

ARTICLEINFO:

Received:
30 July 2025

Accepted:
5 September 2025

Available online:
14 September 2025

✉: I. Khosravi
imankhosravi59@iau.ac.ir

ABSTRACT

In this paper, nano-spinel $ZnCo_2O_4$ was demonstrated excellent adsorption efficiency towards reactive black 5 (RB5) as a reactive dye in aqueous solution. The adsorption studies were carried out at different values of pH, contact time, adsorbent dosages, temperatures and dye concentrations. The investigation of removal kinetics of RB5 indicates that the removal process obeys the rate of second-order kinetic equation. The results indicate that the Langmuir adsorption isotherm fitted the data better than the Freundlich. Finally, the photocatalytic degradation of RB5 was examined. The results of experimental showed that the degradation of RB5 dye follows only an adsorption process.

Keywords: Adsorption, Dyes, Materials, Nanoparticles, Sol-gel process, Photocatalysis.

1. Introduction

In recent years, increasing concern for public health and environmental quality has led to a growth of special interest in developing and implementing various methods of removing potentially toxic organic and inorganic pollutants from water [1]. Dyes from a wide variety of sources, such as textiles, printing, dyeing, dyestuff manufacturing and food plants, are major sources of environmental pollution and recognized as difficult-to-treat pollutants [2]. There exist various classes of dyes, like azo, reactive, acidic, basic, neutral, disperse and direct dyes

[3-5]. The presence of dyes in water reduces light penetration and hinders photosynthesis in plants [6]. Some dyes and their degradation products in surface water are reported to be highly carcinogenic [7]. It is, therefore, essential to treat the dye effluents prior to their discharge into the receiving water. Recently, different methods dealing with treatment of textile wastewater like conventional methods including physico-chemical treatment [8], biological oxidation [9], adsorption [10], chemical oxidation [11], ozonation [12], electrochemical degradation [13], coagulation and membrane treatments [14], have been investigated.

Several types of natural and synthetic adsorbents have been evaluated for the removal of dyes from colored water and wastewater [15]. Among these materials, spinel compound is one of the most widely studied and used adsorbents for environmental pollution control. Spinel compounds have a general formula AB_2O_4, could be considered as an adsorbent/catalyst material for the removal of dyes. Spinels are attractive subjects for continuous scientific interest and have been deeply investigated in material science because of their physico-chemical properties [16].

Gao et al. synthesized magnetic mesoporous spinel $NiFe_2O_4$ of high surface area by a facile oxalate decomposition process [17]. The mesoporous material showed good adsorptive property for the mesoporous material showed good adsorptive property for adsorbent to treat AO7 contained wastewater. Photocatalytic degradation processes have been widely applied as techniques of destruction of organic pollutants in wastewater and effluents. Wu et al. [18] evaluated the effectiveness of magnetic ferrite $CuFe_2O_4$ powder as an adsorbent/catalyst material for the removal of azo-dye acid red B (ARB). They showed magnetic $CuFe_2O_4$ powder processes the excellent adsorptive properties towards azo-dye ARB at pH< 5.5. This study has investigated the efficiency of nanospinels, $ZnCo_2O_4$, as an adsorbent for removal of azo dye, reactive black 5 (RB5), from an aqueous solution. The effect of different variables including contact time, pH, temperature, and dosage of adsorbent was evaluated. Two kinetic models were also analyzed for the removal of RB5 on $ZnCo_2O_4$ nanoparticles. The last aim of the present study is to investigate the photocatalytic decomposition of RB5 in water over $ZnCo_2O_4$ nanoparticles.

2. Experimental procedure

2.1. Preparation of nanospinel

For the preparation of the nanospinel $ZnCo_2O_4$, in this work, the powders of Co $(NO_3)_2.4H_2O$ (0.01 mol, 4.0 g) and Zn $(NO_3)_2.6H_2O$ (0.005 mol, 1.5 g), were dissolved in 35 ml of ethanol and then was added 15 ml to solution included 2:1 mol oxalic acid in ethanol.

The mixture was stirred for 18 h at room temperature which led to the formation of a sol and then evaporated at 70 ºC for 2 h under constant stirring until gel was formed. A viscous gel was obtained which dried at 120 °C and was calcined at 600 ºC for 4 h for obtaining the well-crystallized spinel.

The decomposition and reaction processes of the dried polymeric gel were analyzed by differential thermal analysis DTA, using a NETZSCH, Germany, in the temperature range from room temperature to 1000 °C, in air with a heating rate of 10 °C/min**.**

The nanoparticles were characterized by XRD employing a scanning rate of 0.02 s^{-1} in a 2θ range from 0° to 70°, using a Ẋ pert, 200, Philips, the Netherlands, equipped with CuKα radiation. The data were analyzed using JCPDS standards**.**

The complex polymeric gel and derived powders were also analyzed by Fourier transform infrared (FTIR) spectroscopy on thermo Nicollet Nexus 870 FTIR spectrometer. The morphology and dimension of the nanoparticles were observed by transmission electron microscope which was taken on a LEO 912 AB transmission electron microscope using an accelerating voltage of 120 kV.

2.2. Dye removal experiments

The commercial color index (CI) reactive dye was used without further purification (Table 1). The synthetic of dye solution was distributed into different flasks (1 L capacity) and pH was adjusted with the help of the pH meter (HOBIRA D14E). The initial RB5 dye concentration in each sample was 50 mgL^{-1} after adding 0.01 g of catalyst in 10 ml of the sample. All experiments were conducted at 25 $^{\circ}$C and the pH values 1, 7 and 11.

Table1. Molecular structure of the studied dye.

Dye	Name	Structure	λ_{max} (nm)	M_w
RB5	**Reactive Black 5**	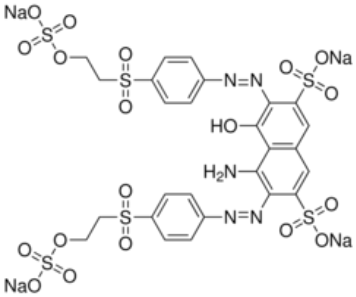	**598**	**991.82**

3. Results and discussion

3.1. Thermal analysis

Figure 1 shows the DTA curve of the $ZnCo_2O_4$ gel precursor obtained by the sol-gel method. The DTA curve shows a large endothermic peak around 150 °C which is assigned to the evaporation of ethanol. The exothermic peak around 320 °C might be due to the combustion of the organic compounds such as oxalic acid and residual ethanol. The small exothermic peak at 410 °C can be attributed to the decomposition of nitrate which decomposes completely around 600 °C and results a large exothermic peak [19]. No obvious change was observed above 600 °C. Hence, it is plausible to conclude that the lowest calcinations temperature is about 600 °C.

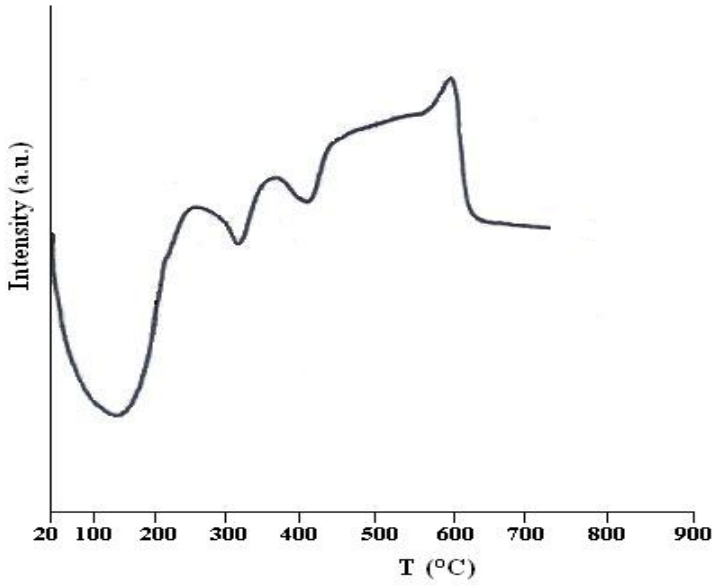

Figure 1. DTA curve of the $ZnCo_2O_4$ precursors obtained by the citric acid –metal nitrate polymerized complex.

3.2. X-ray diffraction studies

Figure 2 shows the X-ray diffraction patterns using CuK_α radiation from the spinel-type $ZnCo_2O_4$ formed when the gel was calcined at 600 °C for 4 h. The diffraction peaks at 2θ angels that appeared at 18.91, 29.05, 36.54, 38.19, 44.31, 55.00, 58.75 and 64.32° can be assigned to scattering from the (111), (220), (311), (222), (400), (422), (511) and (440) planes of the spinel crystal lattice, respectively.

The peaks of XRD spectrum confirm clearly that the phases belong to $ZnCo_2O_4$ and match well with the phase reported in the powder diffraction database [20]. The data of XRD shows $ZnCo_2O_4$ crystallizes in a cubic phase with a = 8.1700 Aº. The crystallite sizes were calculated from the XRD peak broadening of the (311) peak using the Scherer's formula:

$$D_{hkl} = \frac{0.9\lambda}{\beta_{hkl}\cos\theta_{hkl}} \quad (1)$$

where D_{hkl} is the particle size perpendicular to the normal line of (hkl) plane, β_{hkl} is the full width at half maximum, θ_{hkl} is the Bragg angle of (hkl) peak and λ is the wavelength of X-ray. The particle size of $ZnCo_2O_4$ nanoparticles calcinated at 600 °C is about 30 nm.

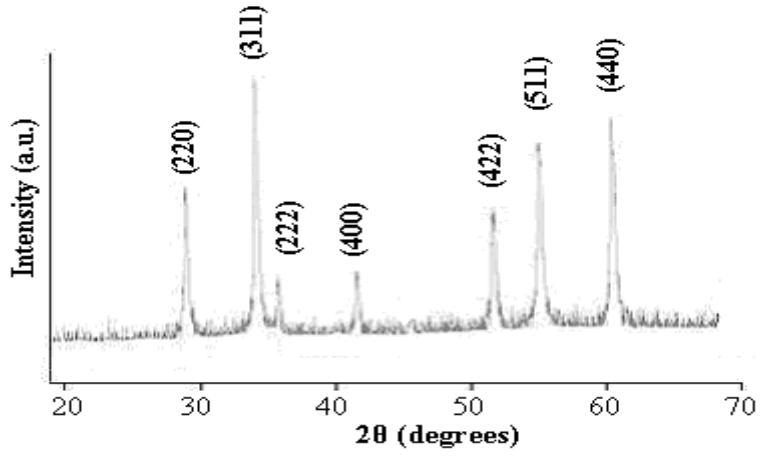

Figure 2. XRD patterns of the $ZnCo_2O_4$ powders sintered at 600 °C.

3.3. IR spectra of dried gel and annealed particles

The vibrations of ions in the crystal lattice are usually observed in the range of 400–700 cm^{-1}. Two main broad metal–oxygen bands are seen in the Far-IR spectra. The highest one, generally observed in 580 cm^{-1}, corresponds to intrinsic stretching vibrations of the metal at the tetrahedral site (T_d), $M_{Td} \leftrightarrow O$, whereas the υ_2, lowest band usually observed in 470 cm^{-1}

which is assigned to octahedral metal stretching (*Oh*), $M_{Oh} \leftrightarrow O$ (Fig. 3a) [21]. The FTIR spectrum (Fig. 3b) reveals that the vibration band of $C-O$ bond shifts from 1110 cm^{-1} for pure oxalic acid to 1085 cm^{-1} for the $ZnCo_2O_4$ nanoparticles which indicate that the oxygen atom from $C-O$ bond coordinates with the metal on the surface of $ZnCo_2O_4$ nanoparticles [22]. The surfactant molecules in the adsorbed state are influenced by the field of solid-state surface. As a result, the characteristic bands shift to the lower frequency regions.

The surfactant has a coordination bond or strong interaction with nanoparticles and thus kinetically controls the growth rates of various faces of crystals and it can control the morphology.

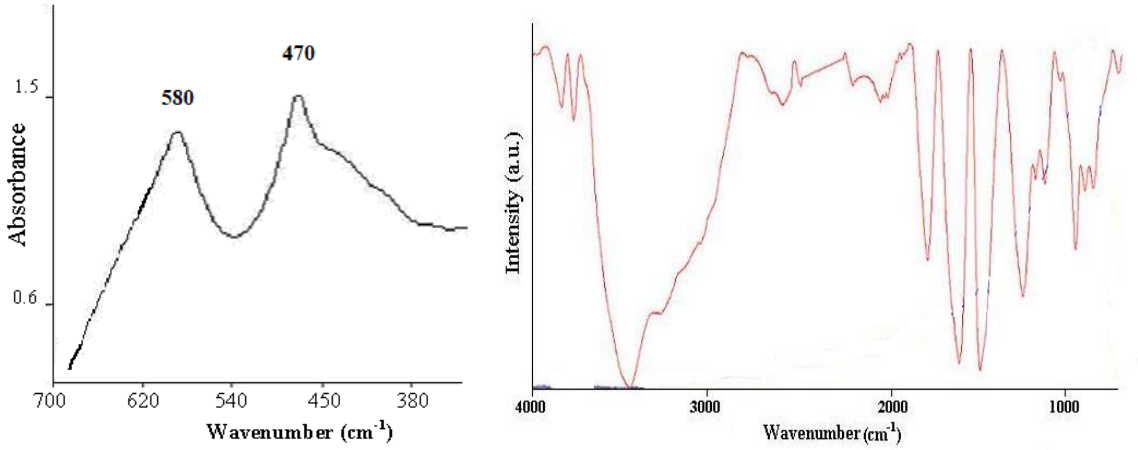

Figure 3. (a) Far-IR spectrum and (**b**) FTIR spectrum of $ZnCo_2O_4$

3.4. Powder morphology

The size of spinel particles was evaluated and conformed by TEM. Figure 4 shows representative TEM image of $ZnCo_2O_4$. The image of the sample which calcined at 600 °C consists of particles ranging in size of about 30 nm. As the TEM images show, the morphology of nanoparticles is homogeneous [23].

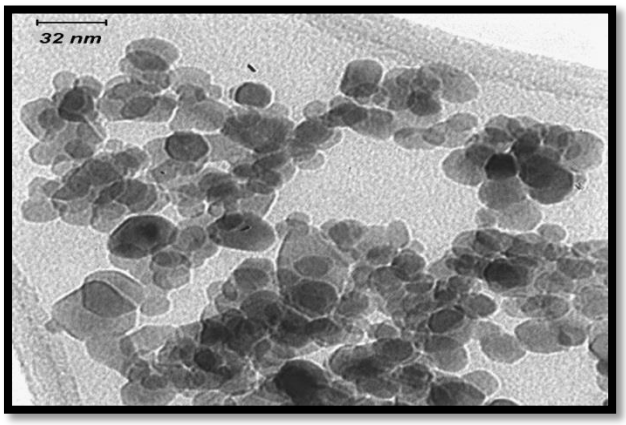

Figure 4. TEM micrograph of $ZnCo_2O_4$ nanoparticles obtained at 600 °C for 4 h with different magnifications.

3.5. Dye removal by $ZnCo_2O_4$ nanoparticles

The efficiency of prepared and characterized $ZnCo_2O_4$ nanoparticles as an adsorbent for removal of RB5 dye from liquid solutions was investigated using a batch equilibrium technique placing different amount of adsorbent in a glass bottle concentrations. The adsorption studies have been carried out for different pH values, contact time, different temperatures and adsorbent doses.

3.6. Effect of pH

Since the solution pH is an important parameter on removal dye molecules [24]. The initial pH of the solution has been changed in the range of 1-11 with a stirring time of 10 min. The initial concentrations of dye and adsorbent dosage were set at 50 mg/L and 0.01 g, respectively. The percentage of dye removal is defined as:

$$\text{Removal rate}\,\% = \frac{C_o - C(t)}{C_o} \times 100 \qquad (2)$$

where C_o and $C_{(t)}$ are the initial concentration and concentration of RB5 dye at time *t*, respectively. The removal of RB5 dye above 94 % was achieved at pH = 1. So this pH was selected to run further experiments (Fig. 5)

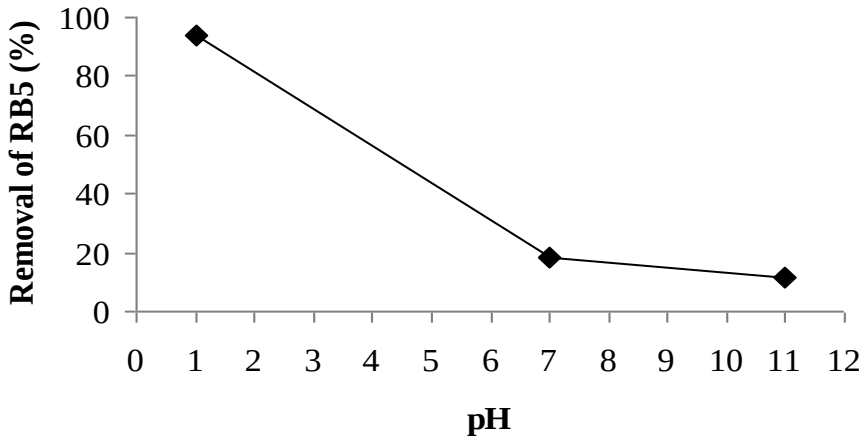

Figure 5. Effect of pH on removal of RB5. Experimental conditions: mass of adsorbent, 0.01 g; initial dye concentration, 50 mgL-1; volume of dye solution, 10 ml; temperature, 25 ºC; time, 10 min.

3.7. The effect of temperature

The removal of RB5 by $ZnCo_2O_4$ nanoparticles was carried out at 15 °C, 25 °C, 35 °C and 45 °C. Increasing temperatures from 15 °C to 45 °C eventuate to increase in the percentage of removal rate from 87.8 to 96 %, respectively. Accordingly, the adsorption of RB5 using nanoparticles is controlled by kinetically process (Fig. 6).

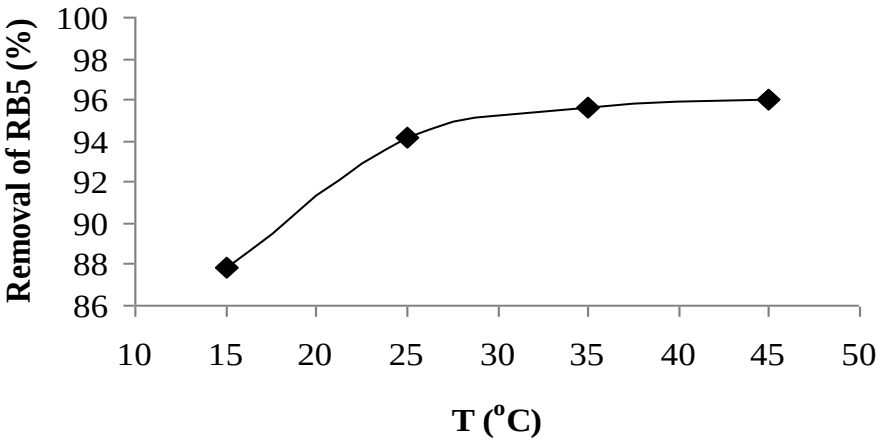

Figure 6. Effect of temperature of RB5 adsorption onto of $ZnCo_2O_4$. Experimental conditions: mass of adsorbent, 0.01 g; initial dye concentration, 50 mgL-1; volume of dye solution, 10 ml; and pH = 1.

3.8. The effect of contact time

The effect of contact time on the removal of RB5 by $ZnCo_2O_4$ nanospinels shows that decrease in the concentration of RB5 dye with time is due to the adsorption of dye on $ZnCo_2O_4$ nanoparticles [25] (Fig. 7).

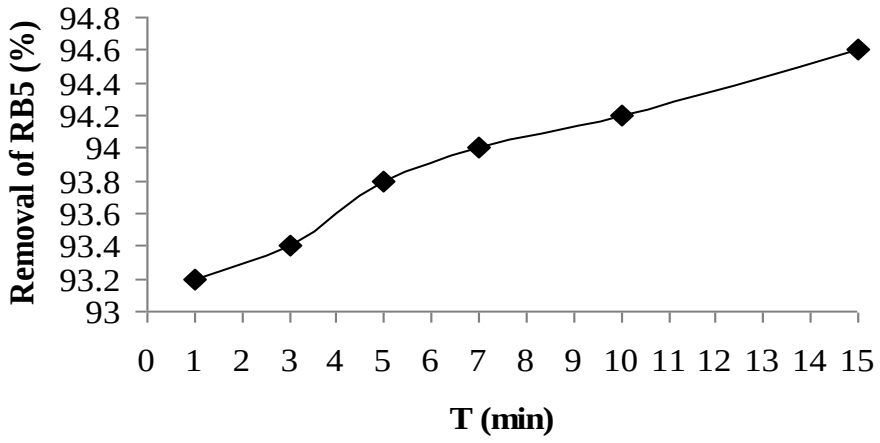

Figure 7. Effect of stirring time on removal of RB5. Experimental conditions: mass of adsorbent, 0.01 g; initial dye concentration, 50 mgL-1; volume of dye solution, 10 ml; temperature, 25 ºC; and pH = 1.

3.9. The effect of $ZnCo_2O_4$ dosage

The effect of $ZnCo_2O_4$ quantity on removal of RB5 dye was investigated in batch experiments by adding various dosage of adsorbent in 0.01, 0.02 and 0.03 g. The results showed that as the adsorbent dose increases, the percentage removal of RB5 dye also increases. This is due to increase the number of contact points in the adsorbent (Fig. 8).

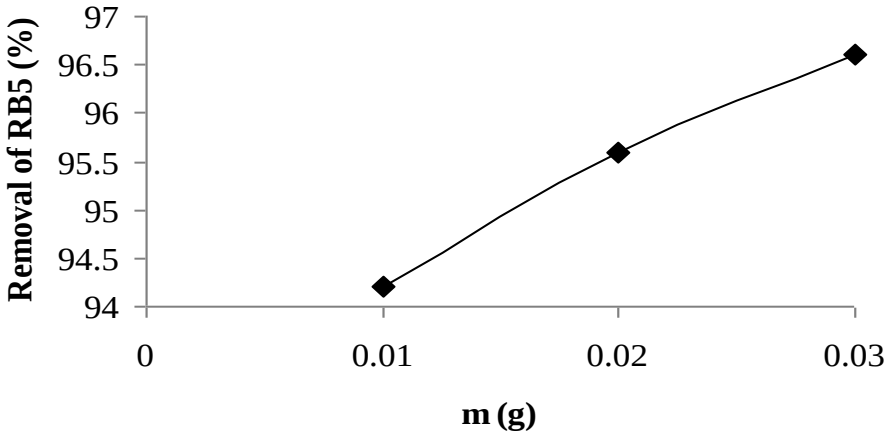

Figure 8. Effect of adsorbent dosage of RB5 adsorption onto of $ZnCo_2O_4$. Experimental conditions: initial dye concentration, 50 mgL-1; volume of dye solution, 10 ml; temperature, 25 ºC; and pH = 1.

3.8. Chemical kinetic removal models

The first-order (Eq. 3) [26] and second-order model (Eq. 4) [27] were provided to test experimental data and to find a suitable chemical removal model for describing experimental data , the obtained data were fitted into the first and second-order models:

The first-order equation: $ln\ C_{(t)} = ln\ C_o - k_1 t$ (3)

The second-order equation: $$\frac{1}{C(t)} = k_2 t + \frac{1}{C_o}$$ (4)

where k_1 and k_2 are the first-order and second-order rate constant, respectively. C_o stands for the initial RB5 concentration and $C(t)$ is the concentration of RB5 at time t. The correlation factor (R^2) for the second-order (Fig. 9) is 0.98 which is higher than that of the first-order model. The results of experimental for the two models show that the removal of RB5 dye is done in second-order kinetic with rate constant of 0.005 $M^{-1}min^{-1}$.

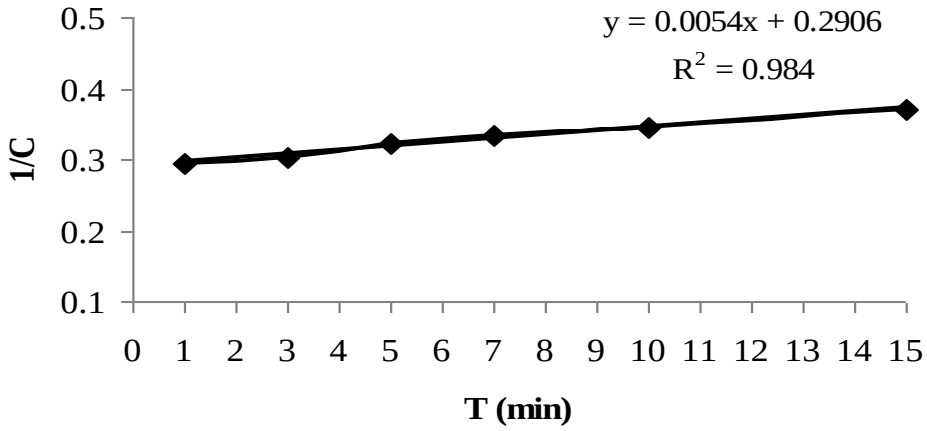

Figure 9. The second-order model. Experimental conditions: mass of adsorbent, 0.01 g; initial dye concentration, 50 mgL-1; volume of dye solution, 10 ml; temperature, 25 ºC and pH = 1.

3.9. Adsorption isotherms

The equilibrium adsorption isotherm model, which is the number of mg adsorbed per gram of adsorbent (q_e) versus the equilibrium concentration of adsorbate, *Ce* is fundamental in describing the interactive behavior between adsorbate and adsorbent. Analysis of isotherm data is so important to predict the adsorption capacity of the adsorbent, which is one of the main parameters required for designing the adsorption system [28]. The equilibrium adsorption isotherm data of RB5 onto adsorbent was analyzed by the Langmuir and Freundlich isotherm models. The amount of dye adsorbed onto $ZnCo_2O_4$ nanoparticles has been calculated based on the following mass balance equation as:

$$q_e = \frac{V(C_o - C_{e)}}{m}$$ (5)

where q_e is the adsorption capacity (mg dye adsorbed onto the mass unit of $ZnCo_2O_4$, mgg^{-1}), V is the volume of the dye solution (L), C_o and C_e (mgL^{-1}) are initial and equilibrium dye concentrations, and m (g) is the mass of $ZnCo_2O_4$ powder added. For the equilibrium

concentration of adsorbate (C_e) and the value adsorbed at the equilibrium (q_e), the following were used forms of the Langmuir (Eq. 6) [29] and Freundlich (Eq. 7) [30] adsorption isotherm equations:

$$\frac{C_e}{q_e} = \frac{1}{bq_{\max}} + \frac{C_e}{q_{\max}} \quad (6)$$

$$\log q_e = \log K_F + \frac{1}{n}\log C_e \quad (7)$$

where the q_{max} (mg g^{-1}) is the surface concentration at mono layer coverage in Langmuir model that represents the maximum amount of q_e. The b parameter is a coefficient related to the energy of adsorption and it increases with increasing strength of the adsorption bond. The values of q_{max} and b can be determined from the linear regression plot of (C_e/q_e) versus C_e. The parameters of the Langmuir equation in this work, namely q_{max} and b are 125 mg/g and 0.347 L/mg, respectively. K_F and n are constants of the Freundlich equation. The constant K_F represents the capacity of the adsorbent for the adsorbate and n is related to the adsorption distribution. A linear regression plot of log q_e versus log C_e gives the K_F and n values that lead to obtained values 1.070 and 3.448, respectively. As Figure 10 (a-b) shows, the value of correlation coefficient (R^2) for Langmuir isotherm is greater than that of the Freundlich isotherm for the adsorption of the dye. This indicates that Langmuir model can describe the adsorption of RB5 dye on $ZnCo_2O_4$ nanospinels better than the Freundlich model, and the dye adsorption occurs as a monolayer onto the homogenous adsorbent surface.

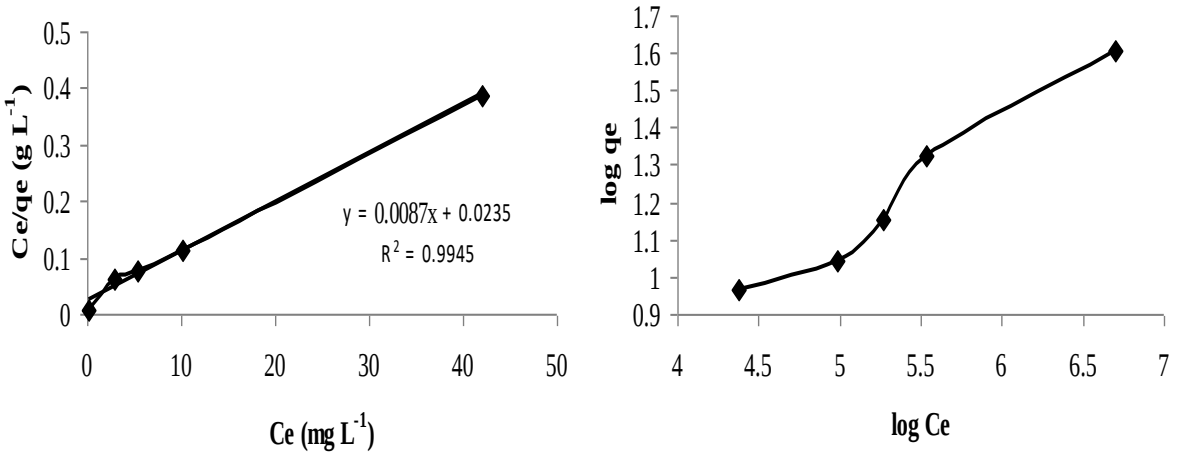

Figure 10. The plot of linearized form of (a) the Langmuir isotherm (b) the Freundlich isotherm. Experimental conditions: mass of adsorbent, 0.01 g; initial dye concentration, 25, 50, 75, 100, 150 mg L-1; volume of dye solution, 10 ml; temperature, 25 ºC; and pH = 1.

3.10. Photocatalytic activity measurement

For the photocatalytic activity measurement, three comparison experiments were performed under the same Conditions, firstly in the presence of catalyst and UV irradiation , secondly in the absence of $ZnCo_2O_4$ catalyst, and thirdly in the dark (Table 2). Since some dyes are degraded by direct UV irradiation [31], it should be examined to what extent RB5 is photolyzed if no photo catalyst was used. In the absence of nanospinels, degradation rates of RB5 under direct UV radiation is only 10 % in 10 min. Obviously the simultaneous utilization of UV irradiation and catalyst could increase the degradation rate of RB5 so that 94 % of RB5 is removed within 1 min. In the presence of catalyst without UV irradiation, the concentration of RB5 decreases quickly at the beginning, and then reaches to a saturation value which is due to adsorption of dye molecules on the surface of nanoparticles. Hence, $ZnCo_2O_4$ nanospinels cannot act as photo catalysts for the degradation of RB5 in an aqueous solution. The degradation is merely an adsorption process.

Table 2. The percentage removal rate of RB5 solution at different conditions.

t (min)	1	3	5	7	10
$ZnCo_2O_4$ + UV irradiation	**94**	**94.6**	**95**	**95.2**	**95.6**
$ZnCo_2O_4$	**93.2**	**93.4**	**93.8**	**94**	**94.2**
UV irradiation	**2.6**	**4**	**6**	**8.2**	**10**

3.4. Thermodynamic parameters

The thermodynamic parameters such as the enthalpy change, ΔH^o, and entropy change, ΔS^o, were estimated at different temperatures according to below equation:

$$\ln K_d = \frac{\Delta S^o}{R} - \frac{\Delta H^o}{RT} \qquad (8)$$

where K_d is the distribution coefficient ($K_d=q_e/C_e$), T is the temperature (K), and R is the gas constant (8.3145 J mol^{-1} K^{-1}). The slope and intercept of the plot of $\ln K_d$ versus 1/T gives the ΔH^o and ΔS^o, respectively.

Furthermore, the values of the standard Gibbs energy change, ΔG^o, were calculated using the following equation:

$$\Delta G^o = \Delta H^o - T\Delta S^o \quad (9)$$

Table 3 shows the standard Gibbs energy change of the RB5 onto $ZnCo_2O_4$. The negative values of the standard Gibbs free energy at various temperatures indicate the spontaneous nature of the adsorption of RB5 from aqueous solutions by $ZnCo_2O_4$ [32]. The positive values of ΔH^o (136.07 kJ mol^{-1}) suggest the adsorption is an endothermic process. The positive values of ΔS^o (451.16 J K^{-1} mol^{-1}) reflect the increasing randomness at the solid/liquid interface during the adsorption of RB5 on the $ZnCo_2O_4$.

Table 3. The standard Gibbs energy change for removal of RB5.

T (°C)	***-ΔG°(kJ mol^{-1})***
15	11.60
25	16.55
35	20.95
45	26.05

4. Conclusions

Spinel $ZnCo_2O_4$ nanoparticles have been fabricated using by the thermal decomposition of Zn–Co gel prepared by sol–gel method in the presence of oxalic acid as a chelating agent. The particle size of nanoparticles is so small in comparison to those, prepared by conventional methods. The adsorption studies have been carried out for contact time, different pH values, different temperatures, and adsorbent doses separately. $ZnCo_2O_4$ nanoparticles have been also proven to removal azo-dye RB5 at pH= 1 effectively. The results show the $ZnCo_2O_4$ nanoparticles can effectively remove high concentrations of RB5 dye molecules. The second-order kinetic model is more successful in representing the experimental data for the removal of RB5 on $ZnCo_2O_4$ nanoparticles. The isotherm modeling reveals that Langmuir equation describes the adsorption of RB5 dye onto the $ZnCo_2O_4$ better than the Freundlich model. Experimental results of the photocatalytic decolorization of the

azo-dye RB5 using $ZnCo_2O_4$ reveal that the decolorization can be achieved by an adsorption process.

References:

[1] A. N. Chowdhury, S. R. Jesmeen, and M. M. Hossain, Removal of dyes from water by conducting polymeric adsorbent, Polym. Adv. Technol., 15, 633-638 (2004).

[2] A. Bhatnagar, and A. K. Jain, A comparative adsorption study with different industrial wastes as adsorbents for the removal of cationic dyes from water. J. Colloid Inter. Sci., **281**, 49-55 (2005).

[3] A. P. Carneiro, R. F. P. Nogueira, and M. V. B. Zanoni, Homogeneous photodegradation of C.I. Reactive Blue 4 using a photo-Fenton process under artificial and solar irradiation, Dyes Pigments, **74**, 127-132 (2007).

[4] S. Song, H. P. Ying, Z. Q. He and J. M. Chen, Mechanism of decolorization and degradation of CI Direct Red 23 by ozonation combined with sonolysis, Chemosphere, **66**, 1782-1788 (2007).

[5] J. Axelsson, U. Nilsson, E. Terrazas, T. A. Aliaga and U. Welander, Decolorization of the textile dyes Reactive Red 2 and Reactive Blue 4 using Bjerkandera sp. Strain BOL 13 in a continuous rotating biological contactor reactor, Enzyme Microb. Tech., **39**, 32-37 (2006).

[6] Y. M. Sloker and M. Le Marechal, Methods of decoloration of textile wastewaters, Dyes Pigments, **37**, 335-356 (1998).

[7] M. A. Brown and S.C. De Vito, Predicting azo dye toxicity, Crit. Rev. Environ. Sci. Technol., **23**, 249-324 (1993).

[8] H. Zhiqiao, L. Lili, S. Shuang, X. Min, X. Lejin, Y. Haiping and C. Jianmeng, Mineralization of C.I. Reactive Blue 19 by ozonation combined with sonolysis: Performance optimization and degradation mechanism, Sep. Purif. Technol., **62**, 376-381 (2008).

[9] L. S. Andrade, L. A. M. Ruotolo, R. C. Rocha-Filho, N. Bocchi, S. R. Biaggio, J. Iniesta, V. Garcıa-Garcia and V. Montiel, On the performance of Fe and Fe, F doped Ti–Pt/PbO_2 electrodes in the electro oxidation of the Blue Reactive 19 dye in simulated textile wastewater, Chemosphere, **66**, 2035-2043 (2007).

[10] G. San Miguel, S. D. Lambert and N. Graham, A practical review of the performance of organic and inorganic adsorbents for the treatment of contaminated waters, J. Chem. Technol. Biotechnol., **81**, 1685-1696 (2006).

[11]M. B. Kasiri and A. R. Khataee, Photooxidative decolorization of two organic dyes with different chemical structures by UV/H_2O_2 process: Experimental design, Desalination, **270,** 151-159 (2011).

[12] A. R. Tehrani-Bagha, N. M. Mahmoodi and F. M. Menger, Degradation of a persistent organic dye from colored textile wastewater by ozonation, Desalination, **260**, 34-38 (2010).

[13] F. Yi, S. Chen and C. Yuan, Effect of activated carbon fiber anode structure and electrolysis conditions on electrochemical degradation of dye wastewater, J. Hazard. Mater., **157**, 79-87 (2008).

[14] A. E. Yilmaz, R. Boncukcuoglu, M. Kocakerim and I. H. Karakas, Waste utilization: The removal of textile dye (Bomaplex Red CR-L) from aqueous solution on sludge waste from electrocoagulation as adsorbent, Desalination, **277**, 156-163 (2011).

[15] S. Karcher, A. Kornmuller and M. Jekel, Screening of commercial sorbents for the removal of reactive dyes, Dyes Pigments, **51**, 111-125 (2001).

[16] X. Lou, X. Jia, J. Xu, S. Liu and Q. Gao, Hydrothermal synthesis, characterization and photocatalytic properties of Zn_2SnO_4 nanocrystal, Mats. Sci. & Eng. A., **432,** 221-225 (2006).

[17] Z. Gao, F. Cui, S. Zeng, L. Guo and J. Shi, A high surface area superparamagnetic mesoporous spinel ferrite synthesized by a template-free approach and its adsorptive property, Microporous & Mesoporous Mats., **132**, 188-195 (2010).

[18]. R. Wu, J. Qu, H. He and Y. Yu, Removal of azo-dye Acid Red B (ARB) by adsorption and catalytic combustion using magnetic $CuFe_2O_4$ powder, Appl. Catalysis B: Environ., **48**, 49-56 (2004).

[19] A. Akbar, M. B. Lakshmi, T. K. Das, M. Ghosh, Spinel ferrites in the photocatalytic and adsorptive remediation of dyes and heavy metals: A review, Journal of Water Process Engineering, 71, 1047259 (2025).

[20] X. Wei, D. Chen and W. Tang, Preparation and characterization of the spinel oxide $ZnCo_2O_4$ obtained by sol–gel method, Mater. Chem. Phys., **103**, 54-58 (2007).

[21] F. Bibi, M. Jamshaid , W.A. Al-onazi , A. Kalsoom, M.A. Hossain, R. Iqbal , S.M. Elshikh, S. Iqbal. Design of Sm-doped $GdFeO_3$/g-C_3N_4 heterostructure Z-scheme photo-catalyst for the elimination of malachite green dye from industrial water. Optical Materials, 160, 116696 (2025).

[22] V. J. P. Vilar, C. M. S. Botelho and R. A. R. Boaventura, Methylene blue adsorption by algal biomass based materials: Biosorbents characterization and process behaviour, J. Hazard. Mater., **147**, 120-132 (2007).

[23] M. Dias, M. C. M.Alvim-Ferraz, M. F.Almeida, J. Rivera-Utrilla and M. Sanchez-Polo, Waste materials for activated carbon preparation and its use in aqueous-phase treatment, J. Environ. Manage., **85**, 833-846 (2007).

[24] P. Pandey, P. Kenchannavar, A. Surenjan. Exploring the potential of cashew nut shell biochar for chlorpyrifos pesticide removal. Chemical Engineering and Processing - Process Intensification, 213, 110307 (2025).

[25] I. Khosravi, M.Yazdanbakhsh, E. K. Goharshadi and A. Youssefi, Preparation of nanospinels $NiMn_xFe_{2-x}O_4$ using sol–gel method and their applications on removal of azo dye from aqueous solutions, Mater. Chem. Phys., **130**, 1156-1161 (2011).

[26] A. Afkhami and R. Moosavi, Adsorptive removal of Congo red, a carcinogenic textile dye, from aqueous solutions by maghemite nanoparticles, J. Hazard. Mater., **174**, 398-403 (2010).

[27] I. Langmuir, The adsorption of gases on plane surfaces of glass, mica and platinum, J. Am. Chem. Soc., **40**, 1361-1403 (1918).

[28] H. M. F. Freundlich, Over the adsorption in solution, J. Phys. Chem., **57**, 385-471 (1906).

[29] M. Yazdanbakhsh, I. Khosravi, E. K. Goharshadi and A.Youssefi, Fabrication of nanospinel $ZnCr_2O_4$ using sol–gel method and its application on removal of azo dye from aqueous solution, J. Hazard. Mater., **184**, 684-689 (2010).

[30] L. Liu, L. Xue, Z. Xu, Y. Lao, X. Deng. Iron-regulated (FeCoNiCuZn) O spinel high-entropy oxides: A magnetically recyclable dark catalyst for efficient dye wastewater treatment, Journal of Alloys and Compounds, 1039, 182827 (2025).

[31] R. Kamal, M. M. Ibrahim, Exploiting mesopores binary metal-cobalt spinel oxides catalysts for future sustainable environmental applications: Hydrogen generation and dyes reduction, Fuel, 387, 134400 (2025).

[32] A. R. Ghazy, H. Mahmoud, M. Bishr, R. Kenawy, F. Elhussiny, O. Hemeda, M. Mostafa, Synthesis, structural, optical and dielectric characterizations of Mn1-xCuxFe2O4 for dye removal in alkaline conditions, Journal of Molecular Liquids, 419, 126798 (2025).